High-Pressure Synthesis and Crystal Structure of a New Strontium Ruthenium Oxide: $Sr_2Ru_3O_{10}$

C. Renard, S. Daviero-Minaud,[1] and F. Abraham

Laboratoire de Cristallochimie et Physicochimie du Solide, URA CNRS 452, ENSCL, Université des Sciences et Technologies de Lille, BP 108, F-59652 Villeneuve d'Ascq Cedex, France

The new ternary oxide $Sr_2Ru_3O_{10}$ has been prepared under hydrothermal conditions (480–650°C, 1800–2100 bars) and characterized by X-ray single crystal diffraction data. The structure was refined in *C2/m* space group with $a = 10.985(3)$ Å, $b = 5.635(1)$ Å, $c = 6.452(6)$ Å, and $\beta = 105.3(4)°$. The structure refinement converged to $R = 0.032$ and $R_w = 0.042$. The ruthenium atoms with a mean oxidation number of 5.33 occupy two sorts of octahedral sites. The first form infinite rutile-like chains parallel to the *b* axis, while the second link these chains together to form layers parallel to (100) plane. The average Ru–O bond distance in the two types of octahedra does not allow assignment of an integral oxidation number to individual Ru ions. The Sr^{2+} cations are located in the interlayer space ensuring the stacking cohesion. The $Sr_2Ru_3O_{10}$ structure can also be described by the stacking of SrO_5 layers. The same stoichiometry is encountered in the barium fluorides $Ba_2M_3F_{10}$ (M = Ni, Cu, or Zn) but the stacking sequence is based on BaF_3 and BaF_7 layers. $Sr_2Ru_3O_{10}$ is the first example of strontium ruthenium oxide with Ru/Sr ratio higher than one. The Sr/Ru ratio is allowed by the existence of SrO_5 layers, which creates 1.5 octahedral sites per SrO_5 layer. © 1999 Academic Press

INTRODUCTION

The synthesis and structures of several Sr-Ru-O system compounds have been reported. The oxides $SrRuO_3$ (1–4) and $Sr_{n+1}Ru_nO_{3n+1}$ ($n = 1$, Sr_2RuO_4 (5), $n = 2$, $Sr_3Ru_2O_7$ (6), and $n = 3$, $Sr_4Ru_3O_{10}$ (7)) contain tetravalent ruthenium, whereas the recently studied $Sr_4Ru_2O_9$ oxide contains pentavalent ruthenium (8). The synthesis of the hydrated Ru^{VI} oxide $SrRuO_4 \cdot H_2O$ was also reported (9) but without any information on its crystal structure. The room-temperature structure of $SrRuO_3$ is orthorhombic (2); it is a distorted pseudo-cubic perovskite of $GdFeO_3$ type. Sr_2RuO_4 crystallizes in the K_2NiF_4 structure type (5,6). The other members of the Ruddlesden–Popper $Sr_{n+1}Ru_nO_{3n+1}$ series ($n = 2, 3$) have similar structure with an increasing

number of Ru–O perovskite-type layers, n. The $Sr_4Ru_2O_9$ structure is made up of chains containing a succession of octahedra and trigonal prisms sharing opposite faces in the sequence two octahedra–one prism. The prisms are empty and the ruthenium atoms occupying the octahedra constitute $[Ru_2O_9]$ isolated dimers (8). All these structure types can be described by the stacking of Sr_nO_m layers (m and n are integers) closely related to the close packed SrO_3 layers. The ruthenium atoms occupy the available octahedral sites between the layers. All the reported Sr–Ru–O compounds have been synthesized under atmospheric pressure. As a matter of fact, $Sr_4Ru_2O_9$, containing Ru^V, was stabilized with the oxidizing agent $KClO_3$ and $SrRuO_4 \cdot H_2O$, containing Ru^{VI}, was prepared by the reaction of potassium ruthenate solution with strontium nitrate. Strontium ruthenium oxides have recently known reviewal interest since the discovery of unconventional superconductivity for Sr_2RuO_4 (10) and studies of magneto-optical properties of $SrRuO_3$ (11).

The aim of this work was to obtain high valence ruthenium strontium oxides. Synthesis under hydrothermal conditions in the pressure range 2 kbars was used since we have recently prepared at 500°C, 1800 bars, $Sr_4Ru_{3.05}O_{12}$, a new member of the hexagonal perovskite family (12). In this paper, we report the synthesis and structural determination of $Sr_2Ru_3O_{10}$, a new mixed valence ruthenium oxide.

EXPERIMENTAL

The synthesis of $Sr_2Ru_3O_{10}$ was carried out using hydrothermal conditions. The starting material is a mixture of initial composition 0.5 mmol $Sr(OH)_2 \cdot 8H_2O$ (99% Prolabo) and 0.25 mmol RuO_2 (99.5% Acros). The reactants were sealed in a gold capsule half full of water, with 1 mg of $MnPO_4 \cdot H_2O$ in order to obtain good oxidizing medium.

The gold capsule, put down in a Novaswiss autoclave, was in pressure equilibrium with supercritical water first at 480°C, 1800 bars during 4 days, then at 630°C, 2100 bars for 7 h. The furnace was then cut off and the autoclave left open

---

[1]To whom correspondence should be addressed.

at room temperature. The product, washed with distilled water and filtered, was not homogeneous. It contains two distinguishable crystalline phases. The major phase, with a 2/1 ratio, was tiny black hexagonal platelet crystals identified as the recently reported oxide: $Sr_4Ru_{3.05}O_{12}$ (12). The current work deals with the structure determination of the black square platelet crystals composing the second phase.

STRUCTURE DETERMINATION

A square plate like crystal of dimensions $\sim 0.04 \times 0.1 \times 0.12$ mm^3 was selected. Preliminary rotation and Weissenberg photographs revealed the $2/m$ Laue symmetry with the monoclinic cell parameters, $a \cong 10.9$ Å, $b \cong 5.6$ Å, $c \cong 6.4$ Å, and $\beta \cong 105°$. The systematic absence for hkl reflections with $h + k = 2n + 1$ revealed a C Bravais lattice and possible space groups $C2/m$, Cm and $C2$. Intensity data were collected on a Nonius CAD4 automated diffractometer at room temperature. Crystallographic and collection data are summarized in Table 1. After locating and centering 25 reflections, the unit cell parameters were optimized by a least-squares refinement (Table 1). Absorption corrections were applied using the analytical method of De Meulenaer and Tompa (13). The linear absorption was first set, considering the $SrRuO_3$ formula and $Z = 4$. It was then adapted to the final composition determined from the structure determination.

The structure was successfully solved in the centrosymmetric $C2/m$ space group by the heavy atom method. The positions of the Sr and Ru atoms were determined from the Patterson function calculation. Two independent ruthenium atoms are located in a 2(a) (0; 0; 0) and a 4(h) (0; $\cong 0.23$; 1/2) site, and strontium atoms occupy a 4(i) ($\cong 0.67$; 0; $\cong 0.14$) site. Refinement of the atomic coordinates yielded $R = 0.143$ and $R_w = 0.203$. Analysis of the difference electron density map allowed the location of the oxygen atoms on three 4(i) sites and one 8(j) site. The refinement of these positions and isotropic thermal factors led to $R = 0.042$ and $R_w = 0.051$. The subsequent Fourier difference synthesis calculation did not show evidence of residual electronic density. The final formula is $Sr_2Ru_3O_{10}$ with $Z = 2$ formulae units per cell, $\mu = 201$ cm^{-1}. Atomic scattering factors for neutral atoms and anomalous dispersion correction coefficients were taken from the International Tables for X-ray Crystallography (14). The final cycles of full matrix least-squares refinement included anisotropic temperature factors of all atoms and secondary extinction correction. They led to the final R factors: $R = 0.032$ and $R_w = 0.042$. Refined atomic coordinates and equivalent isotropic temperature factors are listed in Table 2, anisotropic temperature factors are reported in Table 3, and selected interatomic distances and angles are reported in Table 4.

TABLE 1
Crystal Data, Intensity Measurement, and Structure Refinement Parameters for $Sr_2Ru_3O_{10}$

Crystal data	
System	Monoclinic
Space group	$C2/m$
Cell parameters (Å)	$a = 10.985(3)$, $b = 5.635(1)$, $c = 6.452(6)$ $\beta = 105.3(4)°$
Volume (Å^3)	384.7
Z	2
Calculated density (g.cm^{-3})	5.51

Data collection	
Equipment	Nonius CAD4
λ (Mo$K\alpha$)	0.7107
Scan mode (°)	ω-2θ
Scan width (°)	$1 + 0.34 \times \tan\theta$
θ range (°)	2–33
Standard reflections measured every 2h (no decay)	$4\bar{2}1$ 002 $\bar{4}2\bar{1}$ $2\bar{2}\bar{1}$ $2\bar{2}0$ 200
Recording reciprocal space	$-16 \leq h \leq 16$, $0 \leq k \leq 8$ $-9 \leq l \leq 9$
Number of measured reflections	1611
Number of reflections $I > 3\sigma(I)$	1504
Number of independent reflections	931
μ (cm^{-1}) (for $\lambda(K\alpha = 0,7107)$	201
Limiting faces and distances (cm) from an arbitrary origin	$100 \atop \bar{1}00$ } 0.002
	$010 \atop 0\bar{1}0$ } 0.005
	$001 \atop 00\bar{1}$ } 0.006
Transmission factor range	0.185–0.469
Merging R factor R_{int}	0.043

Refinement	
Number of refined parameters	44
R	0.032
R_w (W = $1/\sigma(F_0)$)	0.042

RESULTS AND DISCUSSION

A perspective view of the $Sr_2Ru_3O_{10}$ structure is shown in Table 5. The ruthenium atoms are in octahedral coordination with two crystallographically independent positions

TABLE 2
Atomic Coordinates and Isotropic Displacement Parameters for $Sr_2Ru_3O_{10}$

Atom	Site	x	y	z	B_{eq} (Å^2)
Ru(1)	2a	0	0	0	0.33(2)
Ru(2)	4h	0	0.2299(1)	1/2	0.29(2)
Sr	4i	0.67081(9)	0	0.1455(1)	0.62(2)
O(1)	8j	$-0.0193(4)$	0.2458(8)	0.1915(7)	0.57(9)
O(2)	4i	0.1918(7)	0	0.116(1)	0.8(1)
O(3)	4i	0.3839(6)	0	0.475(1)	0.5(1)
O(4)	4i	0.8611(6)	0	0.459(1)	0.7(1)

TABLE 3
Anisotropic Thermal Parameters for $Sr_2Ru_3O_{10}$

Atom	U_{11}	U_{22}	U_{33}	U_{12}	U_{13}	U_{23}
Ru(1)	0.0065(5)	0.0032(4)	0.0042(4)	0	0.0036(3)	0
Ru(2)	0.0044(3)	0.0036(3)	0.0042(3)	0	0.0030(2)	0
Sr	0.0068(4)	0.0078(4)	0.0100(4)	0	0.0043(3)	0
O(1)	0.013(2)	0.005(2)	0.004(2)	0.001(2)	0.005(2)	− 0.002(2)
O(2)	0.008(3)	0.017(3)	0.007(3)	0	0.004(3)	0
O(3)	0.003(3)	0.006(3)	0.010(3)	0	0.002(2)	0
O(4)	0.003(3)	0.008(3)	0.014(3)	0	0.003(2)	0

Ru(1) and Ru(2). The edge-sharing $Ru(2)O_6$ octahedra form rutile-like chains $(RuO_4)_\infty$ running along the b axis. These chains are linked together by corner sharing $Ru(1)O_6$ octahedra. One $Ru(1)O_6$ octahedron shares two oxygen atoms of one edge with the summit of two consecutive octahedra of one chain and the two oxygen atoms of the opposite edge with the neighboring chain (Fig. 1). The whole RuO_6 octahedra are forming layers parallel to (001). Two following layers are C-translation related. Interleaving strontium ions connect the layers. The strontium atoms are surrounded by nine oxygen atoms (Fig. 2), seven oxygen atoms belonging to one layer (2.61 Å ≤ Sr–O ≤ 2.84 Å) and the two remaining closely coordinated oxygen atoms (d = 2.54–2.49 Å) to the other layer (Table 4).

Despite their isoformulation, $Sr_2Ru_3O_{10}$ and $Ba_2M_3F_{10}$ (M = Ni (15), Co (16), or Zn (17)) present slightly different crystal structures. The latter also contains octahedral sheets but a double row of corner sharing octahedra separate the rutile chains (Fig. 3). Moreover, dimeric units of edge sharing octahedra link the slabs, generating a tridimensional framework of edge and corner sharing octahedra. The $Ba_2M_3F_{10}$ structure can be described in terms of dense packing of BaF_3 and BaF_7 layers closely related to AO_3 close-packed layers. The $Sr_2Ru_3O_{10}$ structure can also be described in terms of stacking layers. The projection of the structure along the b axis shows Sr_pO_q layers (20$\bar{1}$) parallel, with ruthenium atoms occupying the resulting octahedral sites (Fig. 4). The Sr_pO_q slabs of $Sr_2Ru_3O_{10}$ are built from stripes about three atom rows wide: two oxygen rows and one Sr-O row. The arrangement of the Sr-O line in front of the oxygen line from the neighboring stripe destroys the hexagonal symmetry and the resulting layer stoichiometry is SrO_5. For an easier description an almost orthorhombic cell can be defined with unit cell axis, $\mathbf{a}_0 = \mathbf{a} + 2\mathbf{c}$, $\mathbf{b}_0 = -\mathbf{b}$, $\mathbf{c}_0 = \mathbf{a} - \mathbf{c}$ (Fig. 4). Thus, the framework is constituted by an infinite stacking of SrO_5 slabs, perpendicular to the c_0 axis, with the atom rows parallel to b_0. Six layers with the $A_1A_1'A_2A_2'A_3A_3'$ sequence define the cell. The A and A' layers are distinguished by the strontium atom positions (Fig. 5) and the translation vector $\frac{1}{2}\mathbf{a}_0 + \frac{1}{3}\mathbf{c}_0$ allows a deduction of A_{i+1} from A_i. The formation of the $(Ru(2)O_4)_\infty$

rutile-chains results from the A_i-A_i' stacking; the Ru(1) atoms occupy the octahedral sites created between the A_i' and A_{i+1} slabs. Then, the layers built with the rutile-chains and the Ru(1) octahedra are parallel to the (101) plane of the pseudo-orthorhombic cell.
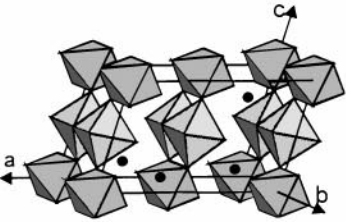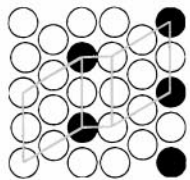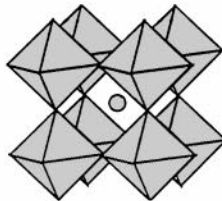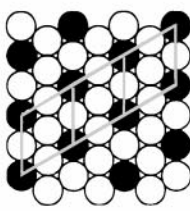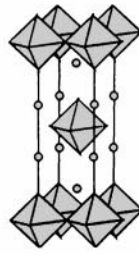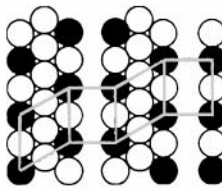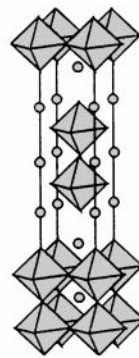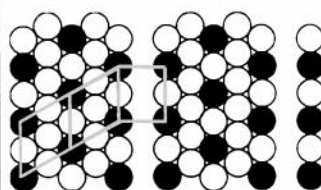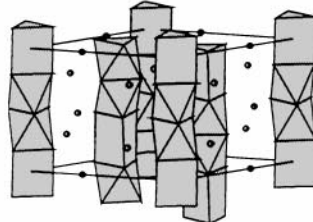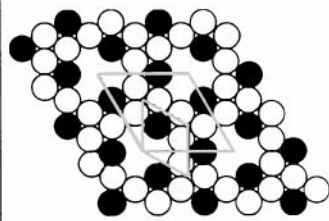
This description allows an easier comparison with the other Sr–Ru–O structures which all can be described by stacking AO_3 layers. Two distinct groups exist. One group with hexogonal symmetry layers like $Sr_4Ru_2O_9$ (8) or

TABLE 4
Interatomic Distances and Selected Bond Angles for $Sr_2Ru_3O_{10}$

Sr polyhedron	Distance (Å)		Angle (°)
Sr–O(1) (2×)	2.613(9)		
−O(1) (2×)	2.761(6)		
−O(2)	2.54(1)		
−O(2) (2×)	2.836(1)		
−O(3)	2.672(9)		
−O(4)	2.488(8)		
		Ru(1) octahedron	
Ru(1)–O(2) (2×)	2.040(7)		
−O(1) (4×)	1.905(5)		
O(1)$_i$–O(1)$_{ii}$	2.769(9)	O(1)$_i$–Ru–O(1)$_{ii}$	93.2(5)
O(1)$_{iii}$–O(1)$_{iv}$	2.769(9)	O(1)$_{iii}$–Ru–O(1)$_{iv}$	93.2(5)
O(1)$_{ii}$–O(1)$_{iv}$	2.62(1)	O(1)$_{ii}$–Ru–O(1)$_{iv}$	87.7(2)
O(1)$_i$–O(1)$_{iii}$	2.62(1)	O(1)$_i$–Ru–O(1)$_{iii}$	87.7(2)
O(1)$_i$–O(2)$_i$	2.852(8)	O(1)$_i$–Ru–O(2)$_i$	95.5(4)
O(1)$_{iv}$–O(2)$_{iii}$	2.852(8)	O(1)$_{iv}$–Ru–O(2)$_{iii}$	95.5(4)
O(1)$_{ii}$–O(2)$_i$	2.852(8)	O(1)$_{ii}$–Ru–O(2)$_i$	95.5(4)
O(1)$_{iii}$–O(2)$_{iii}$	2.852(8)	O(1)$_{iii}$–Ru–O(2)$_{iii}$	95.5(4)
O(1)$_{iv}$–O(2)$_i$	2.728(7)	O(1)$_{iv}$–Ru–O(2)$_i$	87.5(4)
O(1)$_i$–O(2)$_{iii}$	2.728(7)	O(1)$_i$–Ru–O(2)$_{iii}$	87.5(4)
O(1)$_{ii}$–O(2)$_{iii}$	2.728(7)	O(1)$_{ii}$–Ru–O(2)$_{iii}$	87.5(4)
O(1)$_{iii}$–O(2)$_i$	2.728(7)	O(1)$_{iii}$–Ru–O(2)$_i$	87.5(4)
		Ru(2) octahedron	
Ru(2)–O(1) (2×)	1.947(5)		
−O(3) (2×)	1.964(4)		
−O(4) (2×)	1.964(5)		
O(1)$_i$–O(3)$_v^{-100}$	2.75(8)	O(1)$_i$–Ru–O(3)$_v^{-100}$	89.3(4)
−O(3)$_{vii}^{001}$	2.75(8)	O(1)$_i$–Ru–O(3)$_{vii}^{001}$	89.3(4)
−O(4)$_{iii}^{101}$	2.821(6)	O(1)$_i$–Ru–O(4)$_{iii}^{101}$	92.3(3)
−O(4)$_i^{-100}$	2.821(6)	O(1)$_i$–Ru–O(4)$_i^{-100}$	92.3(3)
O(1)$_{iii}^{001}$–O(3)$_v^{-100}$	2.681(6)	O(1)$_{iii}^{001}$–Ru–O(3)$_v^{-100}$	86.7(3)
−O(3)$_{vii}^{001}$	2.681(6)	O(1)$_{iii}^{001}$–Ru–O(3)$_{vii}^{001}$	86.7(3)
−O(4)$_{iii}^{101}$	2.793(8)	O(1)$_{iii}^{001}$–Ru–O(4)$_{iii}^{101}$	91.1(4)
−O(4)$_i^{-100}$	2.793(8)	O(1)$_{iii}^{001}$–Ru–O(4)$_i^{-100}$	91.1(4)
O(3)$_v^{-100}$–O(3)$_{vii}^{001}$	2.48(1)	O(3)$_v^{-100}$–Ru–O(3)$_{vii}^{001}$	78.5(1)
−O(4)$_i^{-100}$	2.827(1)	O(3)$_v^{-100}$–Ru–O(4)$_i^{-100}$	92.0(2)
−O(4)$_{iii}^{101}$	2.827(1)	O(3)$_v^{-100}$–Ru–O(4)$_{iii}^{101}$	92.0(2)
−O(3)$_{iii}^{101}$	2.95(1)	O(4)$_i^{-100}$–Ru–O(3)$_{iii}^{101}$	97.5(2)
Ru(2)–Ru(2)$_{ii}$	2.590(1)		
−Ru(2)$_{ii}^{010}$	3.042(1)		

Note. Symmetry codes: (i) x, y, z; (ii) $x, -y, z$; (iii) $-x, y, -z$; (iv) $-x, -y, -z$; (v) $x + 1/2, y + 1/2, z$; (vi) $x + 1/2, -y + 1/2, z$; (vii) $-x + 1/2, y + 1/2, -z$; (viii) $-x + 1/2, -y + 1.5, -z$.

TABLE 5
Reported Structure of Sr−Ru−O System Compounds

Compound	System and Cell Parameters (Å)	Structure	Sr_nO_m Layer
$Sr_2Ru_2^{V}Ru^{VI}O_{10}$	**Monoclinic C2/m** $a=10.985(3)$, $b=5.635(1)$, $c=6.452(6)$ Å, $\beta=105.3(4)°$		
$Sr_{n+1}Ru_n^{IV}O_{3n+1}$, $n \to \infty$ $SrRuO_3$ (2,3)	**orthorhombic Pbnm** (T<820 K) $a=5.5670(1)$, $b=5.5304(1)$, $c=7.8446(2)$ Å at 300 K **Tetragonal I4/mcm** (820<T<920 K) $a=5.5784(2)$, $c=7.9078(3)$ Å at 823K **cubic Pm3m** (T>920 K) $a=3.9557(1)$ Å at 973 K		
$Sr_{n+1}Ru_n^{IV}O_{3n+1}$, $n=1$ Sr_2RuO_4 (5)	**tetragonal I4/mmm** $a=3.8694(4)$, $c=12.746(2)$ Å		
$Sr_{n+1}Ru_n^{IV}O_{3n+1}$, $n=2$ $Sr_3Ru_2O_7$ (6)	**tetragonal I4/mmm** $a=3.8903(6)$, $c=20.552(5)$ Å		
$Sr_4Ru_2^{V}O_9$ (8)]	**hexagonal P$\bar{6}$2c** $a=9.642(2)$, $c=8.104(2)$ Å		
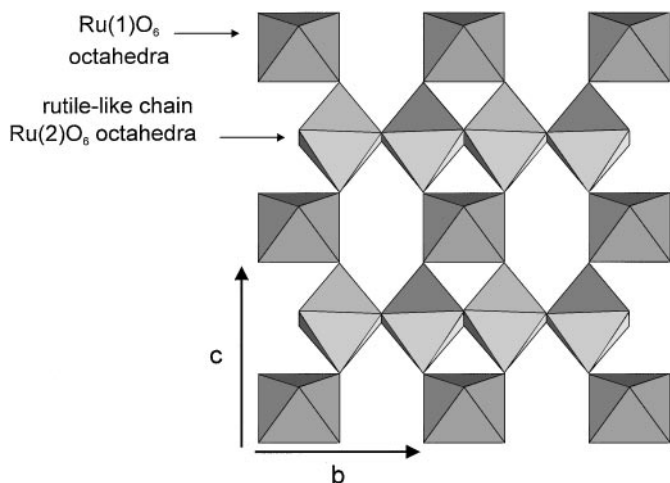
FIG. 1. View of the octahedra layer parallel to (0 0 1) plane in $Sr_2Ru_3O_{10}$, showing the Ru(1) O_6 octahedra linking the $(Ru(2)O_4)_\infty$ rutile-like chains.

FIG. 3. View of the octahedra layer in $Ba_2M_3F_{10}$; the rutile-like chains are separated by two rows of MF_6 octahedra

$SrRuO_3$ (1–4) and another, the $Sr_{n+1}Ru_nO_{3n+1}$ ($n = 1$ (5), 2 (6)) oxides, where there is an arrangement of hexagonal and orthorhombic zones. $SrRuO_3$ adopts an orthorhombic $GdFeO_3$-like perovskite structure, resulting from a staking of compact hexogonal SrO_3 layers (Table 5). $Sr_4Ru_2O_9$ is one example of the $A_{3n+3}A'_nB_{3+n}O_{9+6n}$ series where $n = 3$. The stacking corresponds to mixed AO_3 (A_3O_9) and A_3O_6 layers where three oxygen atoms are replaced by a vacancy (Table 5). Their symmetry is trigonal and the cell symmetry for the $Sr_{n+1}Ru_nO_{3n+1}$ oxides is tetragonal. Their structure is formed by the stacking of Sr_pO_q layers based on perovskite stripes of $2n + 1$ atom rows: $n + 1$ Sr-O rows with n oxygen rows inserted between them. The stripes are separated by a gap of one row wide. The $n = \infty$ compound of this family corresponds to infinite $2n + 1$ stripes and then to $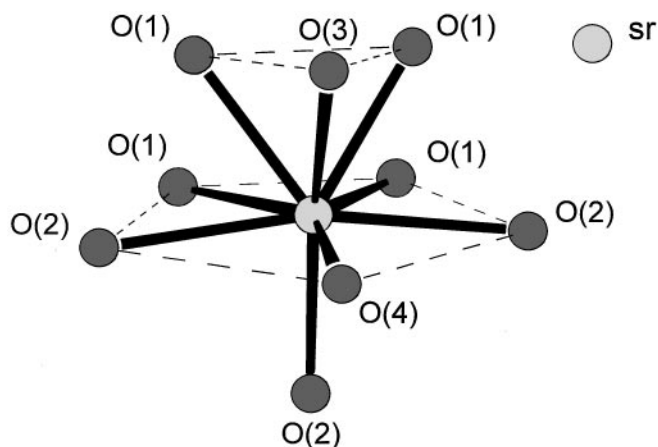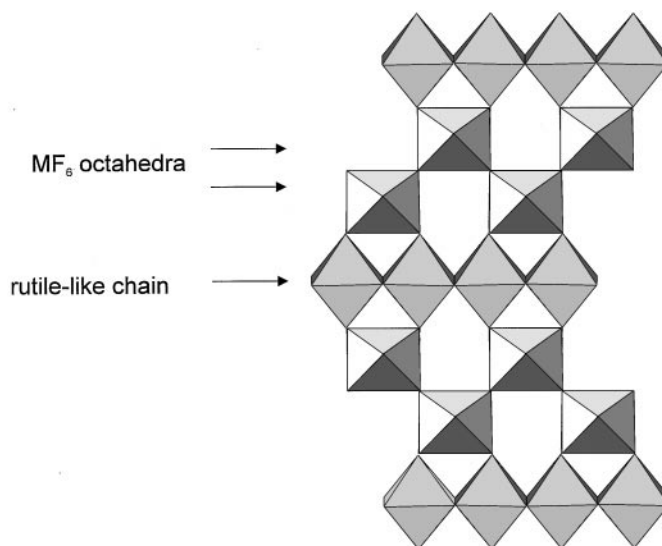SrO_3$ layers, leading to the $SrRuO_3$ distorted perovskite structure. In each case, the coordination of the ruthenium is six-coordinate.

$Sr_2Ru_3O_{10}$ is peculiar in the Sr-Ru-O family because of the Ru/Sr ratio greater than 1. For the other Sr–Ru–O compounds the O/Sr ratio is less than or equal to 3 and this leads to the creation of, at most, one octahedral site between two SrO_q layers. In $Sr_2Ru_3O_{10}$ the O/Sr ratio is equal to 5 resulting in additional octahedral sites. Two sites are located between the A_i and A'_i layers, and another one is created between the A'_i and A_{i+1} layers. On average 1.5 sites are available per SrO_5 layer and in $Sr_2Ru_3O_{10}$ these are fully occupied by ruthenium atoms.

$Sr_2Ru_3O_{10}$ is the first reported strontium ruthenium oxide containing edge-sharing octahedra. These Ru(2) O_6 octahedra are distorted. Along the rutile chains, the Ru–Ru

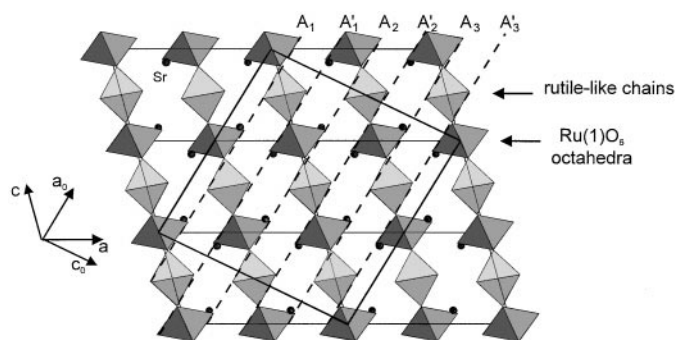**FIG. 2.** Strontium polyhedron coordination in $Sr_2Ru_3O_{10}$.

FIG. 4. Projection along the b axis of the crystal structure of $Sr_2Ru_3O_{10}$, showing the relation between the monoclinic and the pseudo-orthorhombic cell. The black circles are Sr cations inserted between the octahedra layers. The doted lines represent the SrO_5 layers stacking along the c_0 axis of the pseudo-orthorhombic cell.
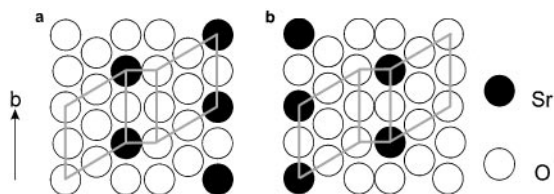
FIG. 5. Representation of the SrO_5 layers in $Sr_2Ru_3O_{10}$. (a) *A* layers, (b) *A′* layers.

distances are alternatively short (2.590(1) Å) and long (3.042(1) Å) with the Ru–O distance remaining close to their mean value (1.96 Å) (Fig. 6). This arrangement is similar to that encountered in the VO_2 (18,19) low temperature structure and in some others MO_2 oxides with a distorted rutile structure.

The short Ru-Ru distance (2.590 Å) across the common edge O(4)–O(4) repulses these, so that O(4)–O(4) distance is noticeably longer (2.95 Å) than the average (2.75 Å). Conversely, the longer Ru–Ru distance (3.042 Å) allows the O(3)–O(3) distance to become shorter (2.48 Å). This last value is shorter than the sum of two O^{2-} ionic radii (20) and is possible evidence of a strong covalent interaction between the O(3) atoms of the edge. It can be compared to the length of the edges sharing octahedra in RuO_2 (2.47 Å) where the Ru–Ru distance is 3.11 Å (21).

In the $Sr_2Ru_3O_{10}$ rutile-like chains, the short metal–metal distance is slightly smaller than the metallic ruthenium one (Ru–Ru = 2.706 Å). That suggests a metallic bonding between the ruthenium atoms across the O(4)–O(4) edge. This is confirmed by the calculation of the α parameter, which provides an estimate of the bond type (22). α is the ratio between the bridging O(4)–O(4) edge distance of the octahedron and the average of the other O–O distances. The metallic interaction across the shared edge of the octahedron displaces the oxygen. This parameter is near 0.9 for the oxides with a rutile-type structure (0.87 for RuO_2) where the metallic atoms have no direct interactions. In the case of a single bond the α value is 1, and it is higher than 1.1 for higher order bond. In $Sr_2Ru_3O_{10}$ chains the α value is 0.89 across the long Ru–Ru distance, which confirms there is no intermetallic interaction. However for the short distance
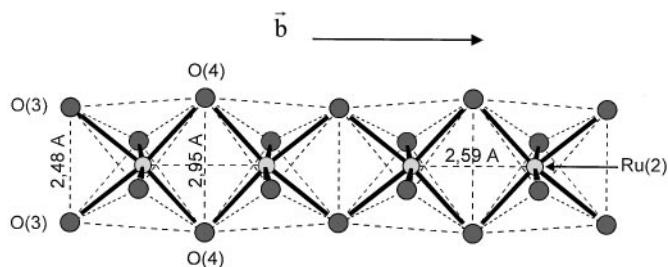
the α value ($\alpha = 1.07$) confirms the metal–metal bonding. Thus, the $Sr_2Ru_3O_{10}$ rutile chains can be described as Ru_2O_{10} dimeric units linked together with the shared O(3)–O(3) edges (Fig. 6). This type of ruthenium dimeric entity, built from two edge-sharing octahedra, is similar to that present in $La_3Ru_3O_{11}$ (23), $Bi_3Ru_3O_{11}$ (24), and $La_4Ru_6O_{19}$ (25), where there are corner sharing Ru_2O_{10} units. In $La_3Ru_3O_{11}$ there is no metal–metal interaction ($\alpha = 0.87$). The Ru–Ru distance is 2.997(1) Å with a shorter common edge 2.474(9) Å for the double octahedra. However $Bi_3Ru_3O_{11}$ and $La_4Ru_6O_{19}$ contain direct Ru–Ru bonding. The O–O shared edge distances are, respectively, 2.98 and 2.997(4) Å, with Ru–Ru distances of 2.60 and 2.488(1) Å, and α values of 1.08 and 1.09, respectively. The observed values in the $Bi_3Ru_3O_{11}$ dimeric units are close to the $Sr_2Ru_3O_{10}$ ones. The Ru(1)–O_6 octahedra are also distorted with four Ru–O distances (1.905(5) Å) shorter than the average (1.95 Å). These oxygen atoms belong to the Ru(2) octahedra. The more distant oxygen atoms (2.040(7) Å) are not shared with other octahedra.

The mean oxidation number of the ruthenium in $Sr_2Ru_3O_{10}$ is 5.33. This nonintegral value brings up the problem of the charge distribution among the ruthenium atoms. Since there are two Ru(2) and one Ru(1), a hypothesis can be put forward assigning the integral oxidation number of 5 for Ru(2) and 6 for Ru(1). However, the average Ru–O diatance in each case is quite similar, namely 1.95 and 1.96 Å, respectively. These values are too close to confirm the distribution. The nonintegral oxidation number can also be explained by postulating some form of charge delocalization along the layers, by interaction across the Ru(1)–O–Ru(2) bridges.

REFERENCES

1. J. J. Randall and R. Ward, *J. Am. Soc.* **81,** 2629 (1959).
2. C. W. Jones, P. D. Battle, P. Ligtfoot, and W. T. A. Harrison, *Acta Crystallogr. C* **45,** 365 (1989).
3. B. J. Kennedy and B. A. Hunter, *Phys. Rev. B* **58,** 653 (1998).
4. B. C. Chakoumakos, J. E. Nagler, S. T. Misture, and H. M. Christen, *Physica B* **241–243,** 358 (1998).
5. L. Walz and F. Lichtenberg, *Acta Crystallogr. C* **49,** 1268 (1993).
6. H. K. Müller Buschbaum and J. Wilkens, *Z. Anorg. Allg. Chem.* **591,** 161 (1990).
7. G. Cao, S. K. McCall, and J. E. Crow, *Phys. Rev. B* **56,** R5740 (1997).
8. C. Dussarrat, J. Fompeyrine, and J. Darriet, *Eur. J. Solid State Inorg.* **32,** 3 (1995).
9. T. L. Popova, N. G. Kisel', V. P. Karlov and V. I. Krivobok, *Russian J. Inorg. Chem.* **26,** 1613 (1981).
10. S. Nishizaki, Y. Maeno, S. Farner, S. Ikeda, and T. Fujita, *J. Phys. Soc. Jpn* **67,** 560 (1997).
11. IV Solovyev, *J. Mag. Mag. Mat.* **177,** 811 (1998).
12. C. Renard, S. Daviero-Minaud, M. Huvé, and F. Abraham, *J. Solid State Chem.*, in press.
13. J. De Meulenaer and H. Tompa, *Acta Crystallogr.* **19,** 1014 (1965).
14. "International Tables for X-Ray Crystallography," Vol. IV, Kynocj Press, Birmingham (1968).

FIG. 6. Representation of the $(Ru(2)O_4)_\infty$ rutile-like chain in $Sr_2Ru_3O_{10}$. The shared O-O edges are alternately long and short.

15. M. Leblanc, G. Ferey, and R. De Pape, *J. Solid State Chem.* **33,** 317 (1980).
16. M. Samouel, *Rev. Chim. Miner.* **8,** 533 (1971).
17. H. G. Von Schnering, *Z. Anorg. Allg. Chem.* **353,** 13 (1967).
18. J. B. Goodenough, *J. Solid State Chem.* **3,** 490 (1971).
19. J. Molenda and A. Stoklosa, *Solid State Ionics* **36,** 43 (1989).
20. R. D. Shannon, *Acta Crystallogr. A* **32,** 751 (1976).
21. C. E. Boman, *Acta Chem. Scand.* **24,** 116 (1970).
22. D. B. Rogers, R. D. Shannon, A. W. Sleight, and J. L. Gillson, *Inorg. Chem.* **8,** 841 (1969).
23. F. Abraham, J. Tréhoux, and D. Thomas, *Mater. Res. Bull.* **13,** 805 (1978).
24. F. Abraham, D. Thomas, and G. Nowogrocki, *Bull. Soc. Fr. Mineral. Cristallogr.* **98,** 25 (1975).
25. F. Abraham, J. Tréhoux, and D. Thomas, *Mater. Res. Bull.* **12,** 43 (1977).